THE ASTROPHYSICAL JOURNAL, 407:175–184, 1993 April 10

OH ZEEMAN OBSERVATIONS OF DARK CLOUDS

R. M. CRUTCHER,[1] T. H. TROLAND,[2] A. A. GOODMAN,[3] C. HEILES,[4] I. KAZÈS,[5] AND P. C. MYERS[3]

Received 1992 August 3; accepted 1992 October 7

ABSTRACT

We have made measurements with the Green Bank 43 m telescope of the Zeeman effect in the 1665 and 1667 MHz lines of OH toward dark clouds. The typical 1 σ sensitivity was 3 μG. The only certain detection of a magnetic field was toward B1, for which we measured a line-of-sight component $|\boldsymbol{B}|\cos\theta = -19.1 \pm 3.9$ μG. Comparison with our earlier measurement of the field toward B1 with the Arecibo telescope provided evidence for a 40% enhancement in field strength between the molecular envelope and core of the B1 cloud, which is consistent with quasi-static contraction of the cloud driven by ambipolar diffusion. Because the Zeeman effect is only sensitive to the line-of-sight component of the magnetic field, a statistical analysis of the detection and upper limits was necessary. This analysis indicated that the total (not line-of-sight) field strength was typically $|\boldsymbol{B}| \approx 16$ μG toward the central regions of dark clouds sampled by the Green Bank beam (for which $A_v \approx 5$ mag and $n_{\rm H} \sim 10^3$ cm^{-3}), which implied that the central regions were approximately magnetically critical. The data were found to be consistent with the hypotheses that (1) dark clouds are in approximate virial equilibrium between magnetic and gravitational energy and (2) the supersonic line widths observed in dark clouds are the result of MHD motions such as Alfvén waves. The data were also consistent with detailed physical models of initially magnetically subcritical clouds evolving on the ambipolar diffusion time scale.

Subject headings: ISM: clouds — ISM: magnetic fields — ISM: molecules

1. INTRODUCTION

The importance of magnetic fields in the evolution of dense interstellar clouds and in the star formation process has become increasingly clear in recent years (see, for example, reviews by Mouschovias 1987, 1991a, b; Shu, Adams, & Lizano 1987; Heiles et al. 1992; McKee et al. 1992). Unfortunately, the experimental difficulty of measuring magnetic field strengths in molecular clouds has severely limited the empirical data base with which to confront the theoretical results. This paper reports very sensitive observations, capable of detecting fields at about the 10 μG level, toward core positions in dark interstellar dust clouds.

The only currently viable technique for measuring the strengths of magnetic fields in interstellar clouds is to detect the Zeeman effect in spectral lines arising in the clouds. The Zeeman effect as first detected in the interstellar medium in H I (Verschuur 1969). However, in dense clouds hydrogen is almost entirely in molecular form; H I Zeeman observations probably probe the field in the low-density, atomic halos of such clouds. One possible exception to this is the observation of the Zeeman effect in H I self-absorption. Heiles (1988) mapped the magnetic field in the vicinity of the dark cloud L204 with this technique. Still, the best way to measure field strengths in molecular clouds is to observe the Zeeman effect for lines which sample the density regime of interest. OH has the advantage over H I of being a molecular species which better samples dense clouds, although it is not an ideal tracer of H_2. OH Zeeman observations should be sensitive to magnetic fields in dark clouds, but possibly not to fields in the highest density cores of molecular clouds. Molecular lines such as those of CN and SO at millimeter wavelengths which have a Landé g-factor comparable to those of H I and OH and which are only observed in high-density regions would seem to be better candidates than OH for probing the densest regions. Unfortunately, the much higher frequencies of these lines lead to a much-reduced sensitivity to magnetic fields.

Crutcher et al. (1975) obtained upper limits to the field strength of 50 μG in the dark clouds ρ Ophiuchi and Heiles Cloud 2. After it was realized that the sensitivity would be much higher if observations were made in *absorption* with a very large telescope, Crutcher, Troland, & Heiles (1981) were able to reduce the upper limits to $\sim$20 μG in the Taurus dark cloud complex toward 3C 123 and 3C 133. The first detection of the Zeeman effect in nonmasing lines of OH was in absorption toward Orion B molecular cloud (Crutcher & Kazès 1983). Since then, the Zeeman effect has been detected in OH absorption lines toward five additional warm molecular clouds with embedded H II regions (W3, Kazès & Crutcher 1986; Orion A, Troland, Crutcher, & Kazès 1986; S88B and W40, Crutcher, Kazès, & Troland 1987; S106, Kazès et al. 1988) and in dark clouds aligned by coincidence with the background continuum sources W22 (Kazès et al. 1986; Heiles & Stevens 1986), Cas A (Heiles & Stevens 1986), and W49B (Crutcher et al. 1987). Finally, as part of our dark cloud project, we (Goodman et al. 1989) detected the Zeeman effect in the OH emission lines toward the dark cloud B1 with the Arecibo telescope.

Although the weakness of OH emission lines toward dark clouds compared to absorption lines produced by a strong background continuum source reduces the sensitivity of Zeeman-effect measurements, the importance of assessing the strengths of magnetic fields in nearby, well-studied dark clouds led us to carry out an extensive, long-term project at the

[1] Department of Astronomy, University of Illinois, 1002 West Green Street, Urbana, IL 61801.
[2] Department of Physics and Astronomy, University of Kentucky, Lexington, KY 40506.
[3] Harvard-Smithsonian Center for Astrophysics, 60 Garden Street, Cambridge, MA 02138.
[4] Astronomy Department, University of California, Berkeley, CA 94720.
[5] Observatoire de Paris-Meudon, Place Jules Janssen, F-92195 Meudon Cedex, France.

NRAO[6] Green Bank 43 m telescope to do just that. This paper reports those results.

2. OBSERVATIONS OF THE ZEEMAN EFFECT

Let $T(v - v_0)$ be proportional to the intensity as a function of frequency v of a spectral line, θ be the angle between the line of sight and the magnetic field, and v_Z be the shift in frequency due to the Zeeman effect. Then for the normal Zeeman effect Table 1 gives the intensities which would be observed with detectors sensitive to left-circularly polarized radiation (T_l), right-circularly polarized radiation (T_r), linearly polarized radiation parallel to $\boldsymbol{B}$ projected onto the sky ($T_\parallel$), and linearly polarized radiation perpendicular to $\boldsymbol{B}$ projected onto the sky ($T_\perp$). With the normalization used in Table 1, the Stokes parameter $I = 8T(v - v_0)$. For the 1420 MHz line of H I and the 1667 and 1665 MHz lines of OH, the Zeeman splitting factors $2v_Z/B = 2.80$, 1.96, and 3.27 Hz μG^{-1}, respectively. If the line width $\Delta v \ll v_Z$, then the three Zeeman components are cleanly separated. In this case observations of T_l, T_r, or $T_\parallel$ will show three lines with shapes given by $T(v - v_0)$ and intensities given by the resuts in Table 1. The direct measurement of the separations v_Z will give the total field strength, and the relative intensities will allow θ to be derived. If both of the linearly polarized components $T_\parallel$ and $T_\perp$ are observed, the orientation of the field on the plane of the sky can also be derived. Unfortunately, non maser lines always have $\Delta v \gg v_Z$, and full information about magnetic fields in extended clouds cannot generally be obtained from Zeeman observations.

It is also possible to infer information about the magnetic field from the Stokes parameter V, Q, and U spectra. The Stokes parameters may be defined in terms of the quantities T_l, T_r, $T_\parallel$, and $T_\perp$ given in Table 1. Letting ϕ be the position angle of the component of $\boldsymbol{B}$ in the plane of the sky, one obtains the following results:

$$
\begin{aligned}
I &= T_r + T_l = 2T(v - v_0 + v_Z)(1 + \cos^2\theta) \\
&\quad + 4T(v - v_0)\sin^2\theta + 2T(v - v_0 - v_Z)(1 + \cos^2\theta)\,, \\
V &= T_r - T_l = [4T(v - v_0 + v_Z) - 4T(v - v_0 - v_Z)]\cos\theta \\
&= +(dI/dv)v_Z\cos\theta\,, \\
Q &= (T_\parallel\cos\phi + T_\perp\sin\phi) - (T_\parallel\sin\phi + T_\perp\cos\phi) \\
&= 2[-T(v - v_0 + v_Z) + 2T(v - v_0) \\
&\quad - T(v - v_0 - v_Z)](\cos\phi - \sin\phi) \qquad (1) \\
&= -\tfrac{1}{4}(d^2I/dv^2)(\cos\phi - \sin\phi)(v_Z\sin\theta)^2\,, \\
U &= [T_\parallel\cos(45^\circ - \phi) + T_\perp\sin(45^\circ - \phi)] \\
&\quad - [T_\parallel\sin(45^\circ - \phi) + T_\perp\cos(45^\circ - \phi)] \\
&= 2[-T(v - v_0 + v_Z) + 2T(v - v_0) \\
&\quad - T(v - v_0 - v_Z)]2^{1/2}\sin\phi \\
&= -\tfrac{1}{4}(d^2I/dv^2)(2^{1/2}\sin\phi)(v_Z\sin\theta)^2\,.
\end{aligned}
$$

Although it is possible in principle to derive the magnitude $|\boldsymbol{B}|\sin\theta$ and position angle ϕ from observations of Stokes parameters Q and U, in fact the amplitude of the Q and U signals are very low because they depend on the *second* derivative of the I spectrum. In practice, it is not currently feasible to detect Q and U signals due to the Zeeman effect.

For the Stokes parameter V spectrum, the contribution at the unshifted frequency v_0 disappears, and the result for a field of strength $|\boldsymbol{B}|$ oriented at an angle θ to the line of sight is precisely the same as the expression for the V spectrum which would be observed for a field of strength $|\boldsymbol{B}|\cos\theta$ oriented parallel to the line of sight. Thus measuring V yields the component of $\boldsymbol{B}$ which is parallel to the line of sight, $|\boldsymbol{B}|\cos\theta$; the actual strength $|\boldsymbol{B}|$ will in general be higher than the measured value inferred from Stokes parameter V spectra.

The V spectrum is the product of the first derivative of the I spectrum and a scaling factor proportional to $|\boldsymbol{B}|\cos\theta$. The analysis technique followed is to calculate the derivative of the I spectrum by numerically differentiating the observed I spectrum. The scaling factor and its derived error are then proportional, respectively, to $|\boldsymbol{B}|\cos\theta$ and to the mean error in $|\boldsymbol{B}|\cos\theta$.

Very small instrumental polarization effects can be very important for Zeeman work. One effect which is not a problem is a small difference in the gains in the two senses of circular polarization. This effect merely adds a scaled-down image of the I spectrum to the V spectrum, and it may be removed by simultaneously fitting a linear combination of the I spectrum and its derivative to the V spectrum, rather than fitting just the derivative. Much more important is the phenomenon of "beam squint," for which the left and right circularly polarized beams of the telescope point in different directions. Beam squint may be caused by a misalignment of the feed axis with respect to the optical axis of the reflecting surface of the radio telescope. Even though a telescope may have no beam squint when pointed at the zenith, mechanical deformations at other positions may produce a misalignment. Beam squint is important for Zeeman work because the combination of beam squint and a velocity gradient in a cloud will produce a V spectrum identical to the one expected for the Zeeman effect. For example, if beam squint were as large as 1′ (only 5% of the Green Bank 43 m telescope beam diameter at 18 cm wavelength), a velocity gradient of only 0.01 km s^{-1} arcminutes^{-1} (about the lowest that could be measured directly) would produce the same line splitting as the Zeeman effect for $|\boldsymbol{B}|\cos\theta \approx 20$ μG. If both the 1665 and 1667 MHz OH lines are observed, beam squint effects can be distinguished from true Zeeman effects as long as the sensitivity of the V spectra is adequate. This distinction is possible since the Zeeman splitting factors for these two lines are different (in the ratio 5/3, see above). Hence, a true Zeeman effect creates different frequency splittings for the two lines while beam squint creates the same (apparent) splittings.

3. OBSERVATIONS AND RESULTS

The OH Zeeman effect observations were obtained during three observing periods between 1986 and 1988 with the NRAO 43 m telescope using a FET (1986 only) or a HEMT prime-focus dual-channel receiver sensitive to both senses of circular polarization. At 18 cm the telescope beam has a full width at half-power of 18′ and a cold-sky system temperature of 20–25 K. Only the willingness of the NRAO to grant very large amounts of observing time and the extremely high sensitivity of this receiver made these observations possible. The 1024 channel autocorrelator was split into four banks of 256 channels; both the 1665 and 1667 MHz lines were observed in

[6] The National Radio Astronomy Observatory is operated by Associated Universities, Inc., under a cooperative agreement with the National Science Foundation.

TABLE 1

OBSERVED ZEEMAN EFFECT LINE INTENSITIES

POLARIZED INTENSITIES	ZEEMAN COMPONENT		
	$\nu_0 - \nu_Z$	ν_0	$\nu_0 + \nu_Z$
T_l	$T(\nu - \nu_0 + \nu_Z)(1 - \cos\theta)^2$	$2T(\nu - \nu_0)(\sin\theta)^2$	$T(\nu - \nu_0 - \nu_Z)(1 + \cos\theta)^2$
T_r	$T(\nu - \nu_0 + \nu_Z)(1 + \cos\theta)^2$	$2T(\nu - \nu_0)(\sin\theta)^2$	$T(\nu - \nu_0 - \nu_Z)(1 - \cos\theta)^2$
$T_\parallel$	$2T(\nu - \nu_0 + \nu_Z)(\cos\theta)^2$	$4T(\nu - \nu_0)(\sin\theta)^2$	$2T(\nu - \nu_0 - \nu_Z)(\cos\theta)^2$
$T_\perp$	$2T(\nu - \nu_0 + \nu_Z)$	0	$2T(\nu - \nu_0 - \nu_Z)$

both senses of circular polarization simultaneously. For the 1986 and 1988 observations the bandwidth of each bank was 156 kHz, while in 1987 a 78 kHz bandwidth was used. The sense of circular polarization was switched every 4 minutes. The instrumental passband was measured and used to construct I spectra by observing blank sky during times when no dark cloud suitable for Zeeman observations was accessible. In most cases these I spectra are the highest sensitivity OH spectra available toward dark clouds and hence are valuable in their own right. Each day a strongly circularly polarized OH maser was observed briefly to test the system.

Before each of the three observing periods we measured the beam squint by making continuum scans of Cygnus A simultaneously in each sense of circular polarization. The beam squint was less than 1″ independent of the pointing of the telescope. This squint is small enough that spurious effects are extremely unlikely.

The observed I and V spectra are shown in Figures 1*a*–1*j*; the results are given in Table 2. (Our OH results for the two positions in the ρ Oph cloud will be discussed in a separate paper; the OH results are listed in Table 2 so they may be included in our discussion of the statistical implications of the complete Green Bank OH Zeeman data set). Integration times per position ranged from 30 to 60 hr. The values for the magnetic fields are the average of the results from the two OH lines weighted by the error in each value. A negative sign indicates that the field direction is toward the observer. Experience has shown that a minimum signal-to-noise ratio of 3 or 4 is required to be confident that the Zeeman effect has been detected. Hence, the only certain detection was toward B1.

For discussion purposes below we shall need the beam averaged OH column density N_{OH}. It is sometimes assumed that the 1667 and 1665 MHz OH lines are thermalized by collisions in dark clouds. In this case, the common excitation temperature T_e, the two optical depths τ_{OH}, and N_{OH} can be derived directly. However, Crutcher (1979) has shown that these lines are in fact very slightly nonthermally excited and that significant overestimates of N_{OH} may result if the thermal assumption is used. For extinctions in the range $0.4 < A_v < 7$, which includes both diffuse and dark clouds, Crutcher found that $N_{OH}/A_v \approx 8 \times 10^{13}$ molecules cm^{-2} mag^{-1}, $T_e \approx 10$ K, and $\tau_{OH} < 1$. Here we assume $T_e = 10$ K (which implies $\tau_{OH} < 1$ for all our observations) and average the slightly different results we obtain separately for the 1665 and 1667 MHz lines. We take the brightness temperature of the background continuum (including the cosmological contribution) to be 4 K except for L889, where we measure 24 K. The N_{OH} we derive are not very sensitive to the precise values of the excitation temperature and background continuum temperature so long as the lines are optically thin. Results for N_{OH} are given in Table 2. Excluding L1647 and L889, which may have more than one cloud along the lines of sight (see § 4.2), $N_{OH} \approx 4 \times 10^{14}$ cm^{-2} for a single cloud. This N_{OH} implies $A_v \approx 5$ mag—typical of the central regions of dark clouds, for which $n(H_2) \sim 10^3$ cm^{-3}. These observations are therefore sensitive to magnetic fields in such central regions, but not in the dense, small cores detected in NH_3 (e.g., Myers & Benson 1983). The NH_3 cores will generally not contribute significantly to the OH spectra because of beam dilution and contributions to the OH lines from the lower density regions surrounding the NH_3 cores.

4. DISCUSSION

4.1. *Theoretical Background*

The most fundamental question addressable by observations is whether magnetic fields are strong enough to have important

TABLE 2

LINE-OF-SIGHT COMPONENT OF MAGNETIC FIELDS IN DARK CLOUDS

Cloud	α_{1950}	δ_{1950}	T_{1665} (K)	T_{1667} (K)	V_{LSR} (km s^{-1})	ΔV (km s^{-1})	N(OH) (10^{14} cm^{-2})	$\lvert B\rvert_{virial}$ (μG)	$\lvert B\rvert_A$ (μG)	$\lvert B\rvert \cos\theta \pm 1\,\sigma$ (μG)
B1	03^{h}30^{m}12^s	+30°57′	0.32	0.54	6.6	1.4	3.9	23	17	−19.1 ± 3.9
L1495W	04 10 01	+28 02	0.33	0.60	6.6	1.0	3.0	18	12	+5.2 ± 2.5
Taurus 16	04 15 01	+28 16	0.45	0.96	7.3	1.0	4.4	26	12	+0.6 ± 2.2
Taurus G	04 28 55	+24 19	0.29	0.49	5.8	1.3	3.2	19	16	+7.5 ± 3.0
L1521	04 30 05	+26 13	0.50	0.78	6.1	1.0	4.2	25	12	−0.4 ± 2.7
TMC1	04 38 47	+25 34	0.47	0.70	5.7	1.5	5.7	34	19	+2.0 ± 3.7
L1647	05 38 50	−07 58	0.61	0.70	4.7	2.3	10.3	30	20	−4.7 ± 3.5
L134	15 50 55	−04 31	0.28	0.44	2.7	0.7	1.7	10	8	−2.6 ± 3.3
L183	15 51 30	−02 44	0.24	0.46	2.4	0.6	1.3	8	7	−1.0 ± 5.1
ρ Oph No. 1	16 24 16	−24 27	0.52	0.87	3.6	1.4	6.4	38	17	+9.5 ± 3.0
ρ Oph No. 2	16 24 30	−24 11	0.26	0.44	3.4	1.3	3.0	18	16	+1.3 ± 4.3
L889	20 25 24	+39 56	−1.00	−1.86	0.3	2.1	8.2	24	19	−0.6 ± 2.1

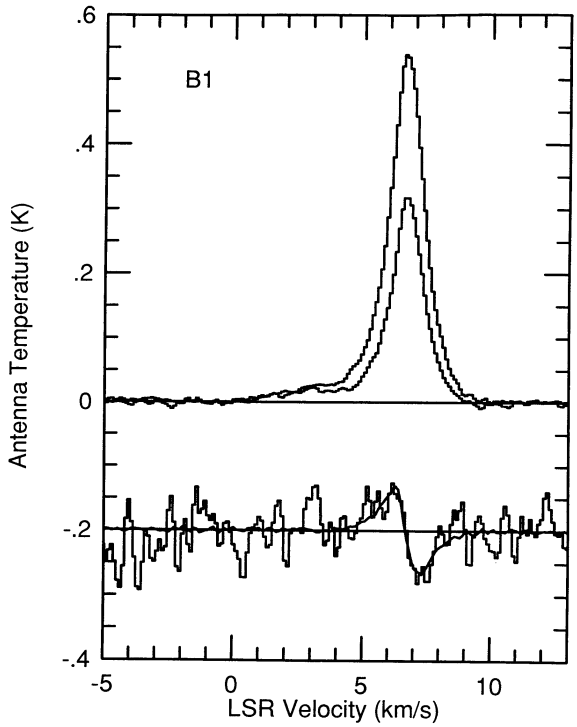

FIG. 1a

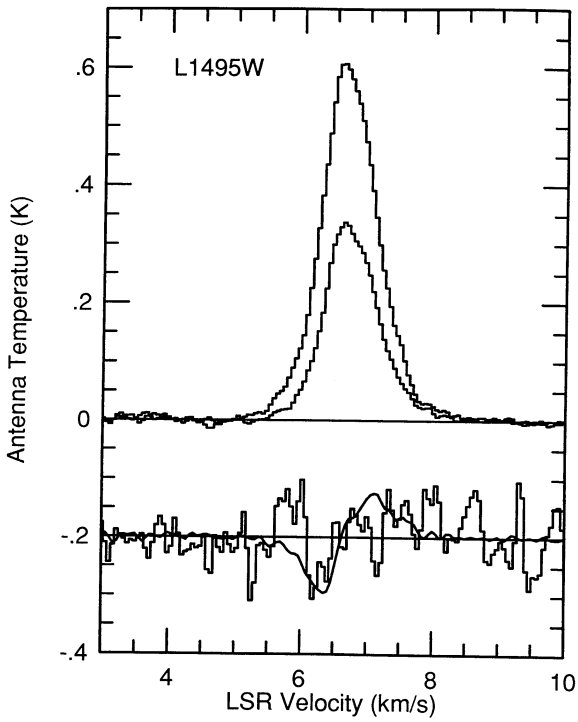

FIG. 1b

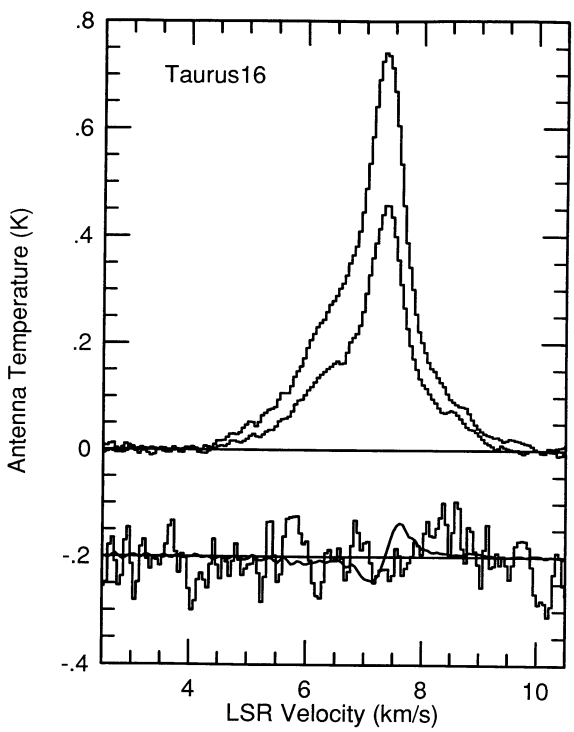

FIG. 1c

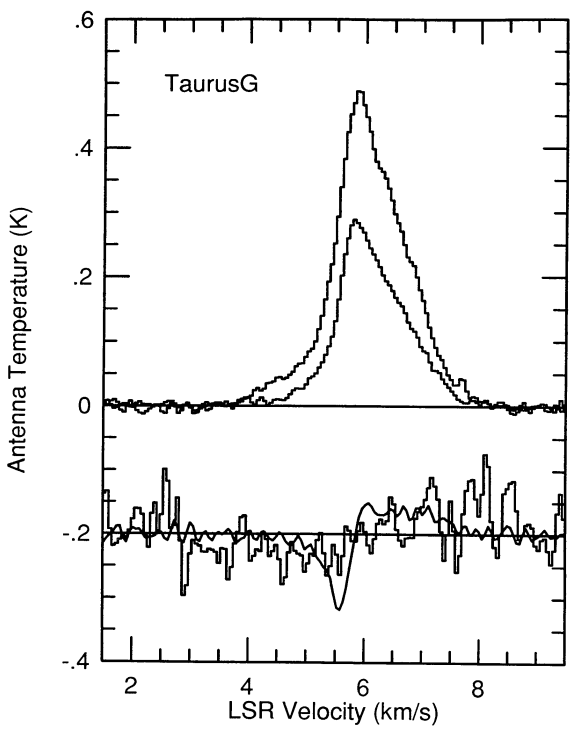

FIG. 1d

FIG. 1.—The Stokes parameter $I/2 = (L + R)/2$ spectra for the 1667 MHz (stronger line) and 1665 MHz lines of OH are plotted together as histograms with the baseline at zero. The average (see text) Stokes parameter $V = R - L$ spectra have been multiplied by 10 and plotted as histograms offset from zero for visibility. The superposed smooth line is the derivative of the Stokes parameter I spectrum. For B1 (*a*) the derivative is scaled for a magnetic field of -19.1 μG. For the other sources (*b–j*) the derivative is scaled for the upper limit to the field strength, $|\boldsymbol{B} \cos \theta| + 3\sigma$.

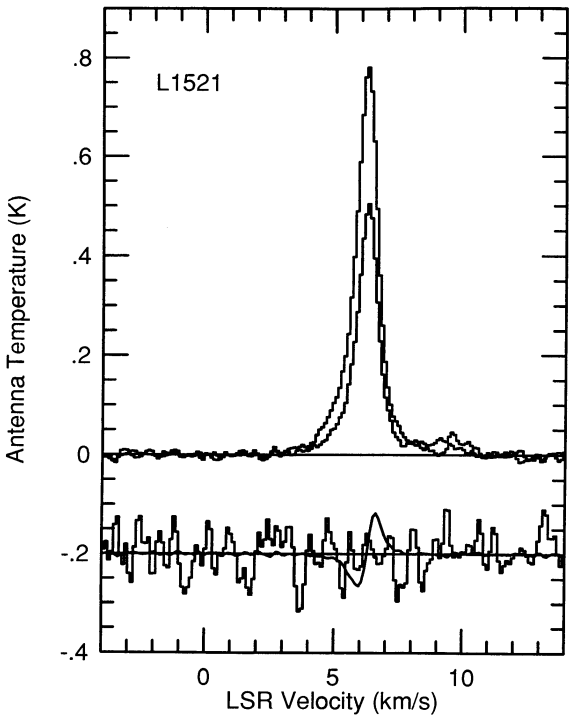

FIG. 1*e*

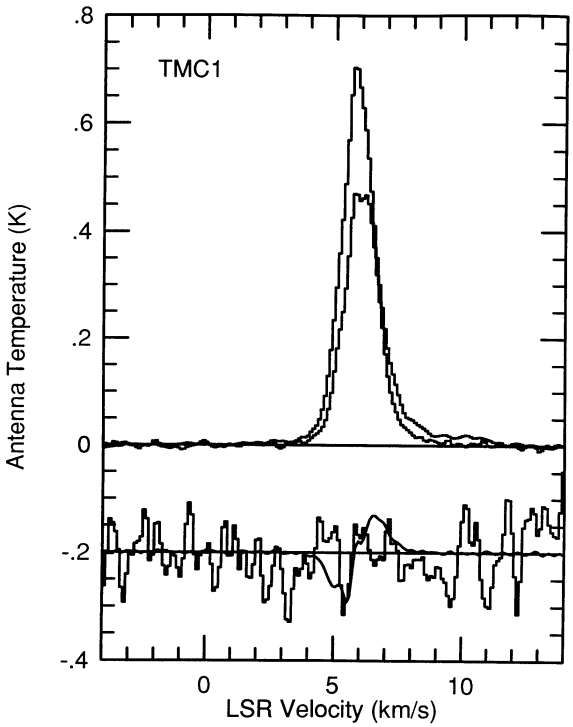

FIG. 1*f*

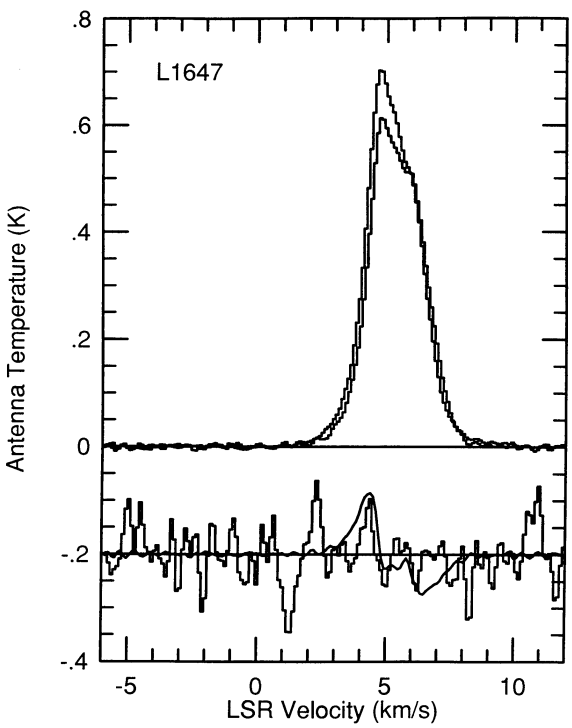

FIG. 1*g*

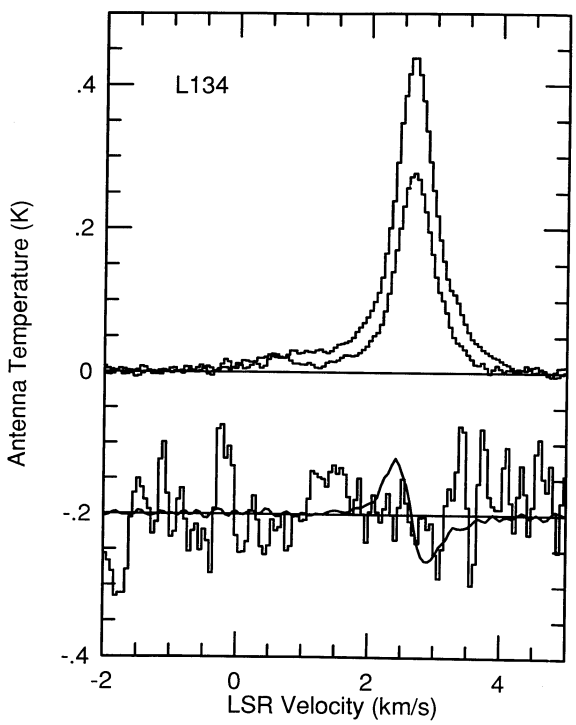

FIG. 1*h*

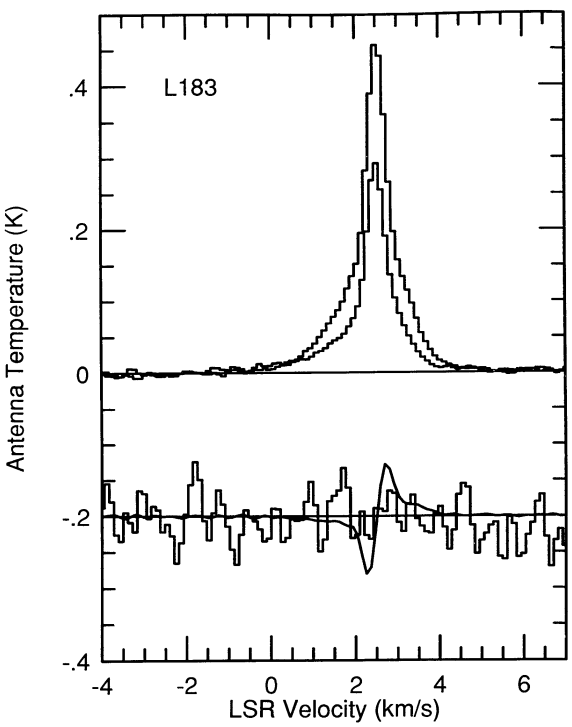

FIG. 1*i*

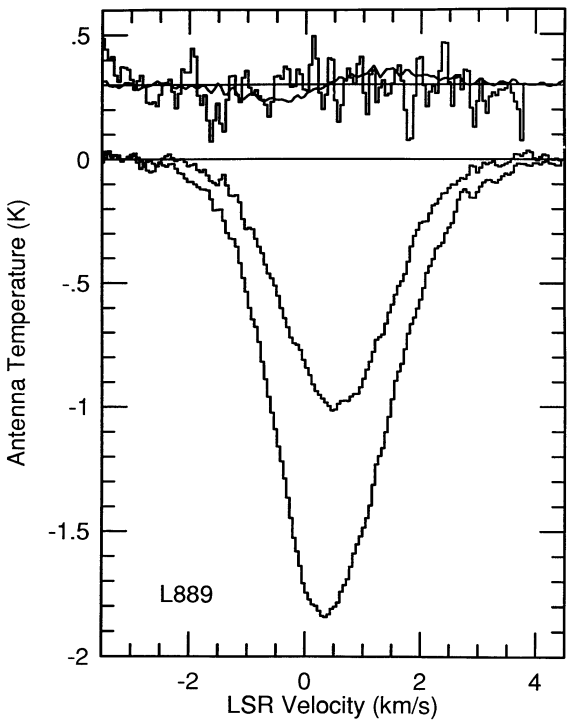

FIG. 1*j*

dynamical effects upon interstellar clouds. It is well known that thermal pressure provides negligible support to self-gravitating dark clouds of the type we have observed. The mass of a typical dark cloud condensation is of order $10^3\ M_\odot$, yet the Bonner-Ebert critical mass for a dark cloud supported by thermal pressure is only $\sim 10\ M_\odot$ (e.g., Mouschovias 1991a). At the same time, these clouds are not observed to be collapsing or rotating; and supersonic turbulence is strongly damped by shocks and therefore cannot persist for a significant fraction of cloud lifetimes. However, there are two additional support mechanisms which are possible if the gas is well coupled to the magnetic field. One is the pressure provided by a large-scale magnetic field. The other is the pressure provided by magnetic field fluctuations on a scale smaller than that of the cloud—fluctuations responsible for supersonic (but sub-Alfvénic) motions. This phenomenon, associated with long-wavelength magnetohydrodynamic (MHD) waves, has a significantly longer damping time scale than supersonic turbulence as long as the fluctuating field strength associated with the MHD waves is less than or comparable to the large-scale, static field strength (Arons & Max 1975; Mouschovias 1987).

A crucial parameter in the discussion of magnetic clouds is the magnetic flux-to-mass ratio, Φ_B/M, which determines the significance of magnetic fields in cloud dynamics and evolution. This parameter can be determined only by observations; and as long as the field is frozen in the matter, it will not change as a cloud evolves. We can use the observations reported here to derive an estimate for Φ_B/M in the central regions of dark clouds.

A simple theoretical approach is to use the virial theorem expressions for the magnetic and gravitational energies for a cloud. If we neglect all other energies and assume equilibrium between magnetic and gravitational energies for a uniform, spherical cloud, we have (Mouschovias & Spitzer 1976):

$$(\Phi_B/M)_{\rm vir} = 3\pi(G/5)^{1/2}\ . \qquad (2)$$

For convenience our subsequent discussion of Φ_B/M will be relative to $(\Phi_B/M)_{\rm vir}$ in the sense

$$\Phi_B/M = k(\Phi_B/M)_{\rm vir}\ . \qquad (3)$$

Although equation (2) depends on specific, simple assumptions, with no loss of generality the quantity k may be used to parameterize cases of nonspherical, non-uniform clouds discussed in the context of the virial theorem (McKee et al. 1992), full numerical models of magnetic clouds (see Mouschovias 1976a, b; Mouschovias & Spitzer 1976; Tomisaka, Ikeuchi, & Nakamura 1988a, b, 1989, 1990; Mouschovias 1991b), or our observational results.

If Φ_B/M is less than a certain value, a cloud is magnetically supercritical and the magnetic field cannot prevent gravitational contraction. If Φ_B/M is greater than this value, the cloud is subcritical and the magnetic field is large enough to prevent gravitational contraction (although ambipolar diffusion can reduce Φ_B/M over time). The exact value of the critical flux-to-mass ratio (i.e., of $k_{\rm crit}$) depends on the spatial variation in flux-to-mass ratio within a cloud (see Mouschovias 1991a; McKee et al. 1992). For example, an *initially* uniform, spherical cloud with a uniform magnetic field will have Φ_B/M lowest in the central flux tube, while an initially uniform cylindrical cloud with uniform magnetic field along the cylinder axis will have Φ_B/M invariant with radius. The latter case will have a lower $k_{\rm crit}$. Mouschovias & Spitzer (1976) and Tomisaka et al. (1988b) found $k_{\rm crit} \approx 1.9$ for physical models of initially uniform, spherical clouds. For any realistic case, $k_{\rm crit}$ is of order unity. Hence, observational determination of k for real clouds is essential for our understanding of the role of magnetic fields in cloud evolution.

For comparison with our observations we transform Φ_B/M into the directly observable magnetic field strength-to-column density ratio $|\boldsymbol{B}|/N$. For a cylindrical flux tube with radius R and average hydrogen column density $N_{\rm H} = N({\rm H\ I}) + 2N(H_2)$

(along the axis of the cylinder), $M = 1.3 m_H N_H \pi R^2$ (allowing for 10% He by number) and $\Phi_B = |B| \pi R^2$, so $\Phi_B/M = (1.3 m_H)^{-1} |B|/N$. Then, using equations (2) and (3), we have $|B|/N_H = 2.4 \times 10^{-21} k$ μG/cm^{-2}. For dark clouds Crutcher (1979) found $N_{OH}/N_H \approx 4 \times 10^{-8}$. Therefore

$$|B|/N_{OH} = 6 \times 10^{-14} k \ \mu\text{G/cm}^{-2} . \quad (4)$$

In Table 2 we list $|B|_{vir}$ computed from N_{OH} and equation (4) with $k = 1$.

Myers & Goodman (1988) investigated whether the supersonic line widths which are observed toward molecular clouds could be the result of MHD motions such as Alfvén waves. Their discussion was in the context of the virial theorem and considered the homogeneous, spherical case rather than detailed physical models of magnetic clouds. Their assumptions were that the virial terms for magnetic energy and self-gravity were equal (which leads to eq. [2]), and that the nonthermal kinetic energy density is equal to the magnetic energy density. The latter assumption leads to $\sigma_{NT}^2 = V_A^2/3$, where σ_{NT} is the nonthermal component of the observed velocity dispersion and $V_A = |B|(4\pi\rho)^{1/2}$ is the Alfvén velocity. For comparison with our Zeeman measurements we assume $T_K = 10$ K and $n_H = 10^3$ cm^{-3}; in Table 2 we list the magnetic field $|B|_A$ implied by this assumption and our measured ΔV. The Zeeman effect is insensitive to the small-scale field $|B|_A$, but the large-scale field that we can measure must be comparable to or greater than $|B|_A$ (Arons & Max 1975; Mouschovias 1987).

The estimates for $|B|_{vir}$ and $|B|_A$ are similar in that each relies on one observable for each position (N_{OH} and ΔV, respectively) and one observationally determined average parameter for dark clouds assumed to apply generally (N_{OH}/N_H and n_H, respectively). The estimates differ in that $|B|_{vir}$ assumes equality of magnetic and gravitational energy, while $|B|_A$ assumes equality of magnetic and kinetic energy. The uncertainties in $|B|_{vir}$ depend linearly on uncertainties in N_{OH} and N_{OH}/N_H; we believe that the uncertainties introduced into the $|B|_{vir}$ values (mainly by uncertainty in N_{OH}/N_H) are less than 50%. The uncertainties in $|B|_A$ depend linearly on uncertainties ΔV and on the square root of uncertainties in n_H. The uncertainties in the observed ΔV are insignificant, but it is likely that n_H varies by factors of several from position to position even if the average value we have assumed is correct. Hence, the uncertainties introduced into the $|B|_{vir}$ values may be as much as a factor of 2 for individual cases; but we believe that the uncertainty on average is less than $\sim 50\%$.

Mouschovias and his group have computed detailed physical models of the evolution of magnetic clouds which may be relevant to dark clouds. As an example, we briefly describe one such model (Mouschovias 1991b) and discuss the implications for our observations. The applicable model clouds are those which are initially subcritical. The model discussed here had an initial equilibrium state parameterized by $n_c = 3 \times 10^3$ cm^{-3}, $|B|_c = 102$ μG, $M = 191$ $M_\odot$, $T = 10$ K, and was subcritical by a factor of 10. We scaled this model downward in central density by a factor of 100 ($|B| \propto n^{1/2}$, $M \propto n^{-1/2}$, and evolutionary time scale $\propto n^{-1/2}$) to be more appropriate for the initial, diffuse H I cloud phase of the evolution of dark clouds; the scaled parameters are $n_c = 30$ cm^{-3}, $|B| \approx 10$ μG, $M = 1900$ $M_\odot$, and $T = 10$ K. The normalized evolution of this subcritical model can then be followed from the Mouschovias (1991b) results. The very slow initial evolution of the model cloud is driven by ambipolar diffusion, for which the time scale is fastest at the core. After 2×10^8 yr the core becomes magnetically critical, with a central density $n_c = 3 \times 10^3$ cm^{-3} and a central magnetic field strength $|B| \approx 15$ μG. However, most of the mass of the cloud would have a magnetic field closer to the original strength of 10 μG, since the field lines in the outer regions of the cloud are approximately "held in place" (Mouschovias 1978) as the central mass-to-flux ratio increases. At this point the evolution of the core speeds up considerably; in another 8 million years the central density will increase by an additional four orders of magnitude and the magnetic field strength by nearly two orders of magnitude as $|B|$ asymptotically approaches scaling as $n_c^{1/2}$. Fragmentation of the core would be initiated by the decay, due to ambipolar diffusion, of MHD waves in the core. These fragments can then collapse and form typically 1 $M_\odot$ stars. Unfortunately, the spatial and temporal scales for core evolution after it becomes critical are too small for our observations to be relevant to these conditions.

After the stage in the evolution of this model when the core approaches becoming critical, the model cloud has a mass, density, temperature, and magnetic field strength which are quite consistent with dark cloud values. The theory makes two predictions that our observations can test. Observations of NH_3 and millimeter-wave lines as well as infrared studies of the core positions we have observed generally show structure in the dense core gas and point infrared sources, which suggest that fragmentation and low-mass star formation has taken place. The relatively large beam size of the 43 m telescope at 18 cm wavelength and the probable decrease in OH/H at high densities (based on astrochemical considerations) cause our Zeeman results to be insensitive to conditions in these very small, contracting fragments. However, over the extended and somewhat lower density central regions which our observations do sample, the predictions are (1) that $|B|$ in the core should have increased by less than a factor of 2 from the original background value, and (2) that $|B|/N$ in the central regions should be near the magnetically critical value (i.e., $k \approx 1$).

In light of this theoretical background, there are three questions that can be addressed by our observations: (1) Are dark clouds in virial equilibrium between gravity and magnetic support (i.e., $k \approx 1$)? (2) Can the supersonic line widths observed in dark clouds be the result of MHD motions such as Alfvén waves? (3) Are evolutionary models of magnetically subcritical clouds (Mouschovias 1991b) applicable to dark clouds? We first discuss the data for the individual clouds and then consider the statistical implications of the observations.

4.2. *Individual Clouds*

B1 was observed at Green Bank after most of the other observations had been completed, primarily because we (Goodman et al. 1989) detected the OH Zeeman effect toward B1 with the Arecibo telescope, which has a beam diameter of $\sim 3'$. The Arecibo result was -27 ± 4 μG. Because the larger Green Bank beam samples primarily more extended regions of the B1 cloud than the Arecibo beam, comparison of the two results offers an opportunity to estimate whether the field is significantly different in the inner and outer core regions of the cloud. The difference of $8 \pm 5\frac{1}{2}$ μG is marginally significant, suggesting that the field is slightly higher in the inner core of the cloud. Such a small (<2) enhancement of the field in the cloud core is a prediction of the originally subcritical model described above (Mouschovias 1991b), for which contraction is driven by ambipolar diffusion.

L1495W, Taurus 16, Taurus G, L1521, and TMC 1 are all cores in the Taurus dark cloud complex. We surveyed OH lines toward a large number of positions selected from lists of NH_3 cores and maps of OH and CO and selected positions for OH Zeeman observations based on these results. Taurus G is not a cloud core position, but was observed because Heiles (unpublished) had tentatively found a field of -18 ± 5 μG in the H I emission line. In none of these cases did we detect the Zeeman effect. (The suggestive results toward L1495W and Taurus G are not detections.) If we hypothesize that there is a uniform magnetic field in the Taurus complex and attempt to derive the best limit to the line-of-sight magnetic field by calculating the weighted average of the five measurements, the result is $|\boldsymbol{B}| \cos \theta = +2.7 \pm 1.5$ μG.

One might consider the negative results in Taurus to be surprising, since there is clear evidence for magnetic fields in the Taurus complex. Several extensive observational studies of linear polarization of background and embedded stars toward clouds in the Taurus complex have been carried out (Hsu 1984; Moneti et al. 1984; Heyer et al. 1987; Goodman et al. 1990) in order to map the direction of the magnetic field in the plane of the sky. Polarization vectors are consistently oriented from star to star within the boundaries of the same cloud, indicating that there is a significant ordered component to the field in Taurus. It is possible that our failure to detect the Zeeman effect in Taurus is due to the field being almost perfectly in the plane of the sky. However, there is direct evidence that the field in Taurus is not invariant in direction; the position angle of the field in the plane of the sky varies by $\sim 60°$ from the northwest part of Taurus near L1495 to the southern part near Taurus G (see Scalo 1990 for a map of polarization vectors over the entire Taurus region). While the field could still be almost perfectly in the plane of the sky throughout Taurus and hence undetectable by the Zeeman effect, that seems unlikely. For example, if the mean field lies in the plane of the sky and its direction varies by 60° in the plane of the sky (i.e., from $\theta = -60°$ to $+60°$), then the observable $|\boldsymbol{B}| \cos \theta$ would range from $-|\boldsymbol{B}|/2$ to $+|\boldsymbol{B}|/2$.

L1647 is part of the Orion molecular ridge and is located $\sim 3°$ south of the Orion nebula. We picked an approximate position based on the OH maps of Baud & Wouterlout (1980), although the exact position we observed for the Zeeman effect was selected on the basis of limited mapping of the OH lines at Green Bank. The observed line profile appears to consist of two velocity components, each ~ 1.3 km s^{-1} wide. If two independent clouds were in the line of sight, for each cloud $|\boldsymbol{B}|_{\rm vir}$ would be reduced by a factor of ~ 2 because of the smaller column densities and $|\boldsymbol{B}|_{\rm A}$ would be lower by a factor of $\sim 2^{1/2}$ because of the smaller line widths. In Table 2 we list these smaller values, applicable to an individual cloud.

L134 and L183 (together with L1778) form a system of high galactic latitude ($b \approx 36°$) dark clouds in Libra which may represent fragments of an original larger cloud (Clark & Johnson 1981). Radial velocity measurements for both L134 and L183 were interpreted by Clark & Johnson as *retrograde* rotation of the cores relative to the outer parts of the clouds, a phenomena predicted by theoretical calculations of the magnetic braking of perpendicular rotators (Mouschovias & Paleologou 1979). Clark & Johnson suggest that magnetic braking of an originally rotating cloud coupled by a magnetic field of 25–100 μG to the surrounding gas could explain the kinematics. We observed L134 and L183 partly in order to try to detect the magnetic field which was hypothesized to have been responsible for magnetic braking. Again, as for the Taurus positions, L134 and L183 are part of the same complex, and the strength and orientation of the field in this Libra dark cloud complex may be constant from position to position. The weighted averaged value of the field in the Libra complex is $|\boldsymbol{B}| \cos \theta = -2.1 \pm 2.8$ μG.

The ρ Oph results will be discussed in a separate paper. The weighted average of the two results is $|\boldsymbol{B}| \cos \theta = +6.8 \pm 2.5$ μG.

L889 has been studied extensively by Dickel, Seacord, & Gottesman (1977) and Wendker, Schramm, & Dieckvoss (1983). They find that L889 is a typical dark cloud complex, with $M \approx 15{,}000$ $M_\odot$, $\langle n \rangle \approx 10^3$ cm^{-3}, $A_V \approx 8$ mag, and $T_{\rm kin} \approx 13$ K. Formation of massive stars has taken place on the back side of the cloud, producing the H II regions IC 1318b and 1318c seen optically on either side of the dark lane produced by L889. Our OH position is near the center of the dark lane. L889 was not included in the sample of Crutcher (1979) and has a slightly higher A_V than those he considered. Since A_V toward L889 was determined by comparison of radio continuum and Hα emission from the H II region behind the dark lane, the cloud provides additional data on the $N_{\rm OH}/A_V$ ratio; for L889 $N_{\rm OH}/A_v \approx 10 \times 10^{13}$ molecules cm^{-2} mag^{-1}, in agreement (within the uncertainties) with the previous result of 8×10^{13} molecules cm^{-2} mag^{-1}. Both $N_{\rm OH}$ and ΔV for L889 are about twice the average values found for the other positions. Because L889 is a dark cloud complex, we shall assume that two clouds are within the Green Bank beam. Hence, as for L1647, in Table 2 we list for $|\boldsymbol{B}|_{\rm vir}$ and $|\boldsymbol{B}|_{\rm A}$ values reduced by 2 and $2^{1/2}$, respectively.

With the exception of L889, all of the cloud positions discussed above are located such that we are looking nearly perpendicularly to the local spiral arm. If the local magnetic field lies along the local spiral arm and if its direction is not significantly affected by the formation of the dark clouds which we are observing, our selection of positions would be significantly biased toward directions where the field lies mainly in the plane of the sky. Since our Zeeman observations are sensitive only to the field component along the line of sight direction, this could explain our lack of detections. The line of sight toward the dark cloud L889, which lies at $l \approx 77.^\circ4$, $b = 1.^\circ0$, is directly down the local spiral arm toward the Cygnus X region. Hence, our observation of L889 allows us to test the hypothesis that magnetic field directions are preferentially along spiral arms. Our extremely low limit to the field strength in L889 argues against the hypothesis that our low detection rate is due entirely to the effect of field orientation. Magnetic fields cannot lie almost perfectly in the plane of the sky everywhere.

4.3. *Statistical Implications*

The results given in Table 2 do not comprise the complete set of Zeeman measurements for dark clouds. However, most of the other measurements have been made with other telescopes toward continuum sources without careful measurements of the antenna temperature produced by the continuum; it is therefore not possible to calculate $N_{\rm OH}$. Moreover, some negative results from programs in which detections have been reported remain unpublished. We choose to use only the uniform sample provided by the Green Bank observations in our statistical discussion of dark cloud OH Zeeman measurements. A possible objection to the validity of our OH Zeeman measurements with the Green Bank telescope is that the relatively large beam (18′) makes it impossible to measure mag-

netic fields in the dense central regions of dark clouds. Our detection of the field in B1 with the Green Bank telescope suggests that telescope beam size is not a significant factor in our failure to detect the Zeeman effect in moderate density ($\geq 10^3$ cm^{-3}) gas toward other dark clouds. Our low upper limit $|B \cos\theta| + 3\sigma \approx 9$ μG toward the TMC 1C core in Taurus from Arecibo OH Zeeman observations (to be published separately) further supports the argument that the large beam of the Green Bank telescope is not responsible for our low detection rate. In any case, the Green Bank observations do correctly measure the OH Zeeman effect for the OH column density contained within the Green Bank beam.

Whether or not our observations are consistent with any theoretical prediction is a statistical question, since we measure $|B|\cos\theta$ rather than $|B|$. For a large sample of measurements with the field directions oriented randomly with respect to the lines of sight, statistically $2|B\cos\theta| = |B|$. Comparison of predicted $|B|_{\rm vir}$ and $|B|_{\rm A}$ values with the observed detection(s) and upper limits in Table 2 and with the average results for cloud complexes discussed in § 4.2 suggest that only B1 is unambiguously consistent with the predictions.

Although there are a number of small potential biases (possible incorrect estimate for $N_{\rm OH}/N_{\rm H}$, contributions to the magnetic energy by small-scale twists to field lines within clouds, the uniform spherical cloud approximation used in the virial theorem, possible velocity gradients within the areas sampled by the Green Bank beam which contribute to ΔV), a more sophisticated statistical treatment of our data is also possible. A measurement of the Zeeman effect with a sensitivity σ can reliably detect a field if $|B\cos\theta| > x\sigma$; our experience suggests that $x = 4$ is certainly safe, and that $x = 3$ is probably reliable. For a random θ the probability P that we would achieve a detection of a field of strength $|B|$ is $P = 1 - (x\sigma/|B|)$ [unless $(x\sigma/|B|) > 1$, in which case $P = 0$]. For each of the hypotheses $|B| = |B|_{\rm vir}$ and $|B| = |B|_{\rm A}$ and for each of the two cases $x = 3$ and $x = 4$, the sum (over the 12 positions) of the individual probabilities P is the predicted number of Zeeman effect detections. These four numbers are given in Table 3 in the column labeled "12 positions." Also given in this column are the percentage probabilities (computed using the binomial distribution) that the hypotheses $|B| = |B|_{\rm vir}$ and $|B| = |B|_{\rm A}$ are consistent with the detection statistics for each of the two cases $x = 3$ and $x = 4$. Although the number of detections is always less than the number predicted, the listed probabilities show that this deficiency is statistically significant only for the $|B|_{\rm vir}$ hypothesis. Therefore, the actual field strengths in dark clouds are apparently less than $|B|_{\rm vir}$ (i.e., $k < 1$), but not necessarily less than $|B|_{\rm A}$.

However, as noted previously, treating all 12 positions as statistically independent may not be justified, if the direction of the field in a cloud complex is correlated from position to position. The fact that the predicted number of detections is much larger than the number of actual detections may therefore be due to bad luck, with the fields at the positions we have observed lying preferentially in the plane of the sky (although our low limit toward L889 argues against this). Instead of assuming that the field directions toward the 12 positions we have observed are uncorrelated, we may consider the opposite extreme and assume that the fields in each dark cloud complex are perfectly aligned (although the variation in the field direction in the plane of the sky in Taurus argues against this assumption). The assumption that fields are aligned within a cloud complex allows us to average results for positions within the same cloud complex. These averaged results were listed in § 4.2 for the Perseus (B1), Taurus (L1495W, Taurus 16, Taurus G, L1521, and TMC 1), Orion (L1647), Libra (L134 and L183), Ophiuchus (ρ Oph 1 and ρ Oph 2), and Cygnus (L889) cloud complexes. The results of this analysis are shown in columns (4) and (5) of Table 3. The predicted numbers of detections remains larger than observed for all cases. However, the percentage probabilities that the observed and predicted numbers are in agreement are sufficiently high for us to conclude that neither the $|B|_{\rm vir}$ or the $|B|_{\rm A}$ prediction is inconsistent with our observations.

TABLE 3

STATISTICAL RESULTS

	12 Positions		6 Complexes	
Item (1)	4 σ (2)	3 σ (3)	4 σ (4)	3 σ (5)
Detections	1	2	1	1
$\|B\|_{\rm A}$, predicted number	2.2	4.1	2.0	2.7
$\|B\|_{\rm A}$, probability	23%	12%	27%	13%
$\|B\|_{\rm vir}$, predicted	5.4	6.6	2.9	3.5
$\|B\|_{\rm vir}$, probability	0.8%	0.7%	11%	4%

It is possible statistically to estimate the strength of the large-scale component of the magnetic field in dark clouds from our data. If we assume that $c \equiv |B|/N_{\rm OH}$ is a constant for the six dark cloud complexes and use a detection threshold of 4 σ, the probability of detection of each complex is $1 - [4\sigma/cN_{\rm OH}]$. Setting the sum of these six probabilities equal to the actual number of detections (1) yields $|B|/N_{\rm OH} \approx 4 \times 10^{-14}$ μG/cm^{-2}. Comparison with equation (4) yields $k \approx \frac{2}{3}$. The fact that $k \approx 1$ implies that the central regions of the dark clouds we have observed are close to being magnetically critical. For a typical (as sampled by the Green Bank beam) dark cloud with $A_V \approx 5$ mag and $N_{\rm OH} \approx 4 \times 10^{14}$ cm^{-2}, the above derived $|B|/N_{\rm OH}$ implies $|B| = 16$ μG. This estimate depends of course on the assumption that $|B|/N_{\rm OH}$ (or equivalently the central magnetic flux-to-mass ratio) is constant from cloud to cloud. It may well be that this is not true. However, this analysis does not depend on the actual *value* of the field detected toward B1. Our derived value $|B|/N_{\rm OH} \approx 4 \times 10^{-14}$ μG/cm^{-2} predicts $|B| = 16$ μG for B1, which is completely consistent with the observed $|B\cos\theta| = 19 \pm 4$ μG if $\theta \approx 0$. This agreement lends support to the above analysis.

5. CONCLUSIONS

We achieved an unambiguous detection of the Zeeman effect toward one of the 12 positions we observed: the B1 cloud in the Perseus dark cloud complex. Previous discussions of the Arecibo measurement of the magnetic field in B1 (Goodman et al. 1989; Heiles et al. 1992) have shown that B1 appears to fit very nicely into the theoretical ideas about magnetic clouds. However, an important question is whether B1 is typical or unusual. Our statistical analysis suggests (but cannot prove) that B1 is not atypical, except in that B in B1 must lie nearly along the line of sight for B1 to be consistent with the other clouds. Our analysis also allowed us to provide some answers to the three questions we posed at the end of § 4.1.

Are dark clouds in virial equilibrium between gravity and magnetic support (i.e., $k \approx 1$)? Our statistical analysis showed that our detection rate was only $\frac{1}{3}$ or less than predicted by the

hypothesis that the clouds are in virial equilibrium between gravitational and magnetic energy. For the 12 positions the probability that this low detection rate could be due to random orientation of the predicted fields is less than 1%. However, this probability became ~10% when the possibility of bias due to correlation in field orientation within a cloud complex was removed by consideration of the six cloud complexes. Moreover, our statistical analysis of the data suggested that $k \approx \frac{2}{3}$. Therefore, we conclude that the data suggest dark clouds are in approximate virial equilibrium between magnetic and gravitational energy.

Can the supersonic line widths observed in dark clouds be the result of MHD motions such as Alfvén waves? Our statistical analysis showed that our detection rate was $\sim\frac{1}{2}$ that predicted by the hypothesis that the dominant nonthermal component of the observed line widths was equal to the Alfvén velocities in the clouds. However, the statistical probabilities of obtaining this result with random orientation of the magnetic field directions, both from position to position and from cloud complex to cloud complex, were ~20% (Table 3). We conclude that the data are not inconsistent with the hypothesis that the supersonic line widths observed in dark clouds are the result of MHD motions such as Alfvén waves.

Are evolutionary models of magnetically subcritical clouds (Mouschovias 1991b) applicable to dark clouds? Although our observations were selectively of central regions of dark clouds with narrow-line NH_3 cores, fragmentation, and point infrared sources, they did not probe the very small core regions which the models would say were supercritical, but instead probed more extended central regions. The models predict that the clouds which have evolved to the stage of collapsing, supercritical cores would be approximately magnetically critical over the areas sampled by our observations, so the theoretical prediction would be $k \sim 1$. Our result $k \approx \frac{2}{3}$, which taken at face value implies that the central regions are slightly supercritical, was consistent with this prediction. In combination with the earlier Arecibo result, our B1 result suggested that the ratio of the field strengths between the central region and the envelope of the dark cloud was ~1.4. This observation supported the theoretical result that a subcritical cloud will evolve quasistatically as the result of ambipolar diffusion, with an increase in the central magnetic field strength by less than a factor of 2. Hence, our data are consistent with the two model predictions which can be addressed. A direct observational test of the prediction that the envelopes of dark clouds are magnetically subcritical ($k > 1$) will be extremely difficult, for although $|\boldsymbol{B}|$ would be only slightly smaller than the core values, the column density N would be several times smaller, reducing the strength of the Stokes I spectra and therefore the sensitivity to $|\boldsymbol{B}| \cos\theta$.

Further understanding of magnetic interstellar clouds will require probing magnetic fields in the very dense central regions which may be undergoing magnetically supercritical collapse, mapping Φ_B/M from envelopes to cores, and comparing these observations directly with detailed physical models. These observational goals are extremely challenging.

This work was supported in part by the following grants from the National Science Foundation: AST8818544 to the Univeristy of California at Berkeley and AST8817651 and AST9116917 to the University of Illinois.

REFERENCES

Arons, J., & Max, C. E. 1975, ApJ, 196, L77
Baud, B., & Wouterloot, J. G. A. 1980, A&A, 90, 297
Clark, F. O., & Johnson, D. R. 1981, ApJ, 247, 104
Crutcher, R. M. 1979, ApJ, 234, 881
Crutcher, R. M., Evans, N. J., II, Troland, T. H., & Heiles, C. 1975, ApJ, 198, 91
Crutcher, R. M., & Kazès, I. 1983, A&A, 125, L23
Crutcher, R. M., Kazès, I., & Troland, T. H. 1987, A&A, 181, 119
Crutcher, R. M., Troland, T. H., & Heiles, C. 1981, ApJ, 249, 134
Dickel, H. R., Seacord, A. W., II, & Gottesman, S. T. 1977, ApJ, 218, 133
Goodman, A. A., Crutcher, R. M., Heiles, C., Myers, P. C., & Troland, T. H. 1989, ApJ, 338, L61
Goodman, A. A., Bastien, P., Myers, P. C., & Ménard, F. 1990, ApJ, 359, 363
Heiles, C. 1988, ApJ, 324, 321
Heiles, C., Goodman, A. A., McKee, C. F., & Zweibel, E. 1992, in Protostars and Planets III, ed. M. Matthews & E. Levy (Tucson: Univ. of Arizona Press)
Heiles, C., & Stevens, M. 1986, ApJ, 301, 331
Heyer, M. H., Vrba, F. J., Snell, R. L., Schloerb, F. P., & Myers, P. C. 1987, ApJ, 312, 855
Hsu, J.-C. 1984, unpublished Ph.D. thesis, University of Texas
Kazès, I., & Crutcher, R. M. 1986, A&A, 164, 328
Kazès, I., Troland, T. H., Crutcher, R. M., & Heiles, C. 1988, ApJ, 335, 263
McKee, C. F., Zweibel, E., Goodman, A. A., & Heiles, C. 1992, in Protostars and Planets III, ed. M. Matthews & E. Levy (Tucson: Univ. of Arizona Press)
Moneti, A., Pipher, J. L., Helfer, H. L., McMillian, R. S., & Perry, M. L. 1984, ApJ, 282, 508
Mouschovias, T. Ch. 1976a, ApJ, 206, 753
———. 1976b, ApJ, 207, 141
———. 1978, in Protostars and Planets, ed. T. Gehrels (Tucson: Univ. of Arizona Press)
———. 1987, in Physical Processes in Interstellar Clouds, ed. G. Morfil & M. Scholer (Dordrecht: Reidel), 453
———. 1991a, in The Physics of Star Formation, ed. C. J. Lada & N. D. Kylafis (Dordrecht: Kluwer), 61
———. 1991b, in The Physics of Star Formation, ed. C. J. Lada & N. D. Kylafis (Dordrecht: Kluwer), 449
Mouschovias, T. Ch., & Paleologou, E. V. 1979, ApJ, 230, 204
Mouschovias, T. Ch., & Spitzer, L., Jr. 1976, ApJ, 210, 326
Myers, P. C., & Benson, P. J. 1983, ApJ, 266, 309
Myers, P. C., & Goodman, A. A. 1988, ApJ, 329, 392
Scalo, J. 1990, in Physical Process in Fragmentation and Star Formation, ed. R. Capuzzo-Dolcetta, C. Chiosi, & A. DeFazio (Dordrecht: Kluwer), 151
Shu, F. H., Adams, F. C., & Lizano, S. 1987, ARA&A, 25, 23
Tomisaka, K., Ikeuchi, S., & Nakamura, T. 1988a, ApJ, 326, 208
———. 1988b, ApJ, 335, 239
———. 1989, ApJ, 341, 220
———. 1990, ApJ, 362, 202
Troland, T. H., Crutcher, R. M., & Kazès, I. 1986, ApJ, 304, L57
Verschuur, G. L. 1969, ApJ, 156, 861
Wendker, H. J., Schramm, K. J., & Dieckvoss, C. 1983, A&A, 121, 69